Electronic Supplementary Information

An ordered organic radical adsorbed on a Cu-doped Au(111) surface

Federico Grillo,[a,*] Herbert Früchtl,[a] Steve M. Francis,[a] Veronica Mugnaini,[b,c] Malena Oliveros,[b] Jaume Veciana[b] and Neville V. Richardson[a]

[a] School of Chemistry, University of St. Andrews, St. Andrews, KY16 9ST, UK

[b] Institut de Ciència de Materials de Barcelona-CSIC, Campus UAB, 08193, Bellaterra, Spain; and Biomedical Research Networking Center in Bioengineering, Biomaterials and Nanomedicine (CIBER-BBN)

[c] present address: Institut für Funktionelle Grenzflächen (IFG), Karlsruhe Institute of Technology (KIT), Hermann-von-Helmholtz-Platz 1 76344 Eggenstein-Leopoldshafen (Germany).

*E-mail: federico.grillo@st-andrews.ac.uk

SI.1 – Experimental details.

Experiments were performed in ultra-high vacuum (UHV) chambers with a base pressure below 5×10^{-10} mbar and equipped with Low Energy Electron Diffraction (LEED) and either Scanning Tunnelling Microscopy (VT-STM, Omicron) or High Resolution Electron Energy Loss Spectroscopy (HREELS, VSW HIB 1000, double pass spectrometer). The Au(111) single crystal was cleaned by argon ion sputtering and annealing cycles until a clean surface, with a sharp $(22\times\sqrt{3})$ LEED pattern and large, flat terraces in STM were observed. Copper was dosed on the Au(111) surface by electrically heating a high purity copper wire wrapped around a tungsten filament, yielding a deposition rate of *ca.* 0.07 ML min^{-1}. The PTMTC radical was sublimed onto the Cu/Au(111) surface in the line of sight direction, by electrically heating a quartz crucible held at *ca.* 435 K, yielding a rate of *ca.* 0.05 ML min^{-1}, as previously calibrated via ex-situ Quartz Crystal Micro Balance experiments.[1] STM images were collected in constant current mode using chemically etched tungsten tips and were processed using the WSxM software package.[2] HREELS measurements were carried out in the specular direction ($\theta_i = \theta_f = 45°$) with a primary beam energy of 4 eV and a typical elastic peak resolution of *ca.* 50 cm^{-1} (6.2 meV FWHM). A maximum likelihood based resolution enhancement method[3] was used to recover the spectra from the instrumental broadening, leading to an improved resolution of *ca.* 40 cm^{-1} FWHM.

SI.2 – Density Functional Theory: Geometrical optimization and Spin Polarized - Density of States (SP-DOS) calculations.

Information on the PTMTC radical spin states was obtained via a series of DFT calculations for four different systems: a free PTMTC radical molecule, a PTMTC-Cu unit, a PTMTC-Cu unit at an inclined angle with respect to an unreconstructed Au(111) surface and a PTMTC-Cu unit standing upright on an unreconstructed Au(111) surface. The different cases are discussed in the following sections. The free PTMTC molecule was initially geometrically optimized using the Gaussian 03 software package,[4] with the B3LYP functional and the 6-311g* basis set. The gold surface was initially optimized using the VASP code,[5] with the PW91 functional,[6] the PAW (Projector Augmented Wave) method using the appropriate pseudopotentials included in the VASP package,[7] a Monkhorst-Pak grid consisting of 15 k-points in each surface direction in the Brillouin zone and an energy cut off of 500 eV, corresponding to 36.75 Ry. The Au(111) surface was modelled as three layers of a 3 × 3 slab and the top-most layer was allowed to relax, with the bottom layers atoms kept fixed at the ideal bulk positions. A vacuum slab equivalent to four metal layers was used to separate the metal slabs in the z-direction. Geometrical optimization and SP-DOS calculations on the molecular networks were carried out using the program SIESTA,[8] employing the PBE functional,[9] a numerical split-valence PAO basis set,[10] with polarization functions (SVP) and Troullier-Martins pseudopotentials,[11] as available from the SIESTA web site. The top gold layer was described using modified strictly localized basis sets, containing diffuse functions, as reported by García-Gil and co-workers.[12]

SI.2.1 Free PTMTC radical molecule.

The optimized geometry and the SP-DOS diagram for the free gas phase PTMTC radical molecule are reported in Figure SI.1a and SI.1b respectively. The SP-DOS diagram shows a Singly Occupied Molecular Orbital (SOMO) level at *ca.* -0.49 eV, in the spin up-state, and a Lowest Unoccupied Molecular Orbital (LUMO) level at *ca.* 0.49 eV, in the spin down-state, leading to a Δ(SOMO-LUMO) = 0.98 eV. $C_{central}$, the central carbon atom, carries *ca.* 39% of the SOMO spin density, the remaining carbon atoms carry *ca.* 43.5%, chlorine atoms *ca.* 10.2% and oxygen atoms *ca.* 7.2%; hydrogen atoms do not seem to contribute to the spin states.

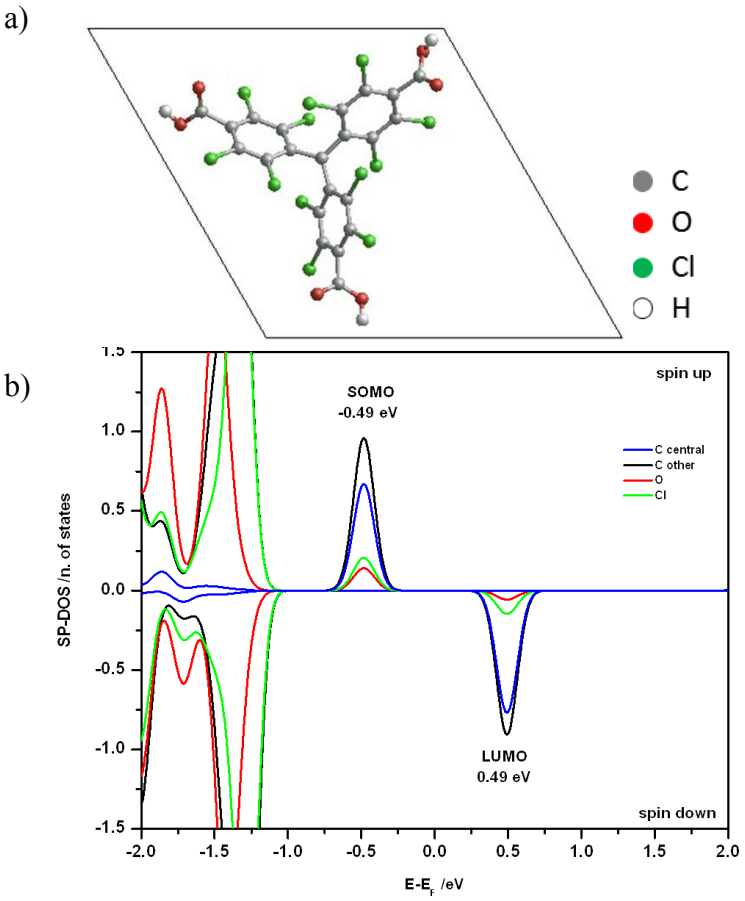

Figure SI.1. a) Free PTMTC radical optimized geometry. b) Free PTMTC radical decomposed SP-DOS diagram.

SI.2.2 Free PTMTC-Cu unit.

The optimized geometry, the SP-DOS diagram for the free PTMTC-Cu unit and the comparison between PTMTC radical and Cu SP-DOS are reported in Figure SI.2. As shown in Figures SI.2b and SI.2c, the copper filled states align with the PTMTC oxygen states at *ca.* -0.9 eV, in both up and down spin states; the copper empty states, however, align with the oxygen spin-up state only (0.55 eV). This allows spin density to be transferred from the oxygen atoms of the carboxylic group to the copper state at *ca.* -0.9 eV.[13]

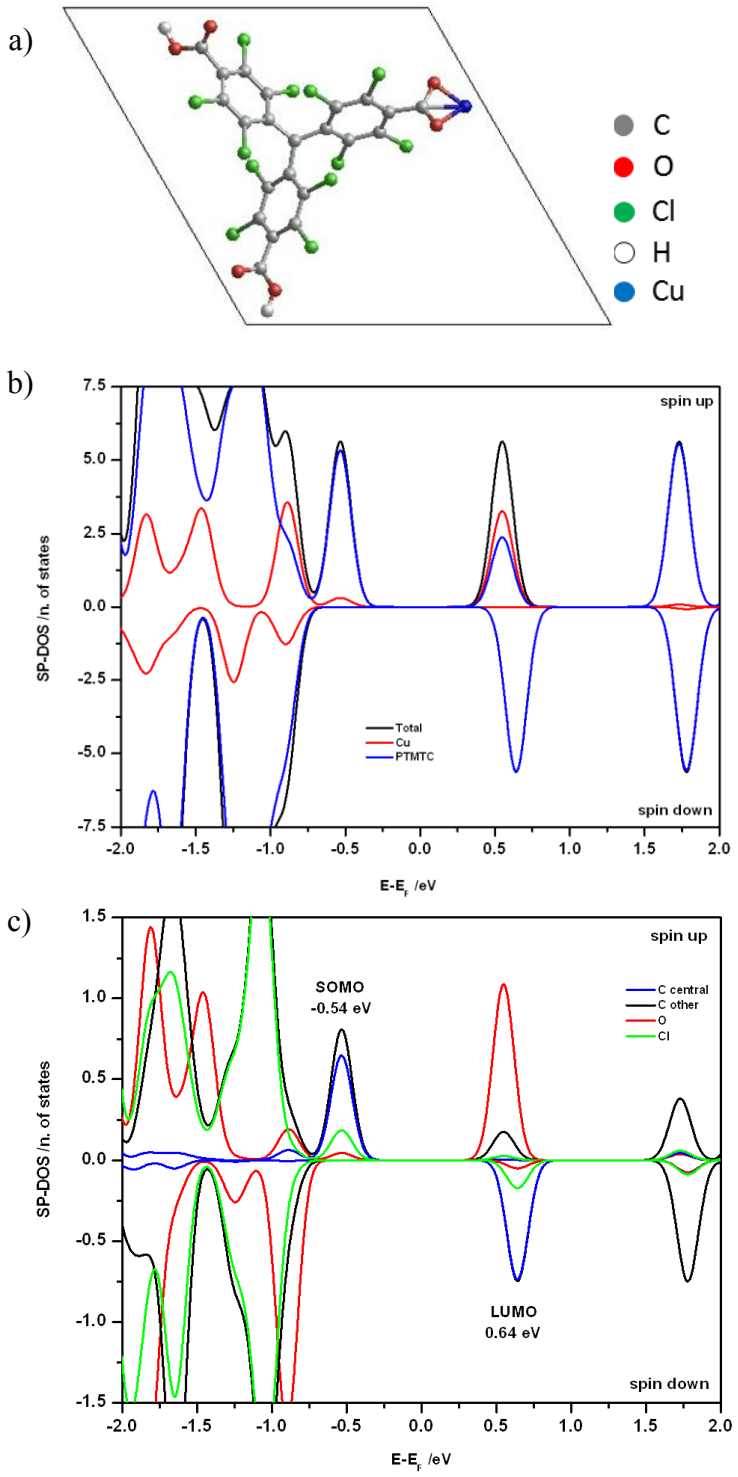

Figure SI.2. a) Free PTMTC-Cu unit optimized geometry. b) SP-DOS contributions for PTMTC, Cu and the whole system are compared. c) Decomposed PTMTC-Cu unit SP-DOS diagram.

As a result, the formerly filled oxygen states are now empty and move up in energy (0.55 eV, Figure SI.2b). Figure SI.2c shows that both oxygen and carbon atoms, belonging to the carboxylic group, contribute to the spin-up state at *ca.* 0.55 eV. Overall charge transfer from

the carboxylic group to the copper occurs; no important changes are seen in the $C_{central}$ or C_{other} states. A SOMO (up) and a LUMO (down) levels are still present and have roughly the same 'composition' as of those of the free PTMTC radical molecule even though they have now shifted in energies, therefore the PTMTC-Cu unit has still a radical character, with a calculated Δ(SOMO-LUMO) = 1.18 eV. Figure SI.3 shows the representations of SOMO and LUMO obtained via Gaussian 03. The SOMO is localized away from the carboxylate end, whereas the LUMO is localized on the copper atom.

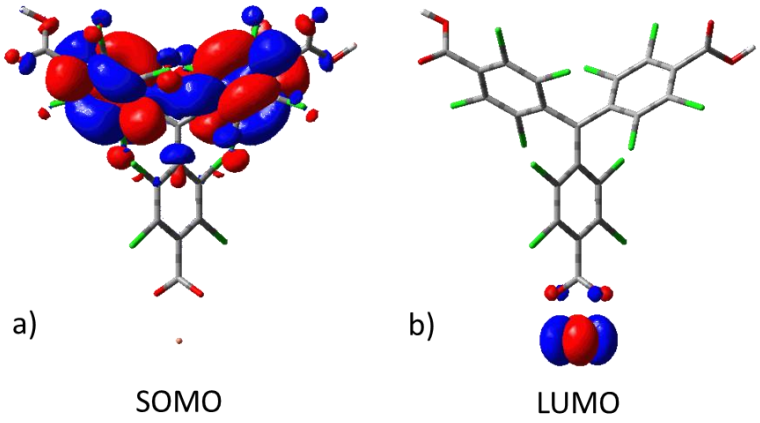

Figure SI.3. SOMO (a) and LUMO (b) molecular orbital contours calculated with Gaussian 03.

SI.2.3 PTMTC-Cu unit inclined at a 15° angle to the Au(111) surface.

Figure SI.4 shows the optimized geometry for a PTMTC-Cu unit on the unreconstructed Au(111) surface. The gold slab consists of 3 layers of 5×5 gold atoms; a vacuum gap corresponding to 10 gold layers was used to separate the slabs in the vertical direction. Optimization of the periodic system shows that a configuration in which the copper atom is shared between two PTMTC molecules is more favorable by *ca.* 0.6 eV when compared to the one in which the copper atom is bound to a single PTMTC molecule. Similarly, geometries in which the Cu-carboxylate section points away from the gold surface are preferred. The molecular plane containing the carbon skeleton, i.e. the plane defined by the $C_{central}$-$C_{bridgedheads}$ atoms, forms a 15° angle with the surface. The dimensions measured on the optimized geometry shown in Figure SI.4b well agree with the experimental values reported in the main text.

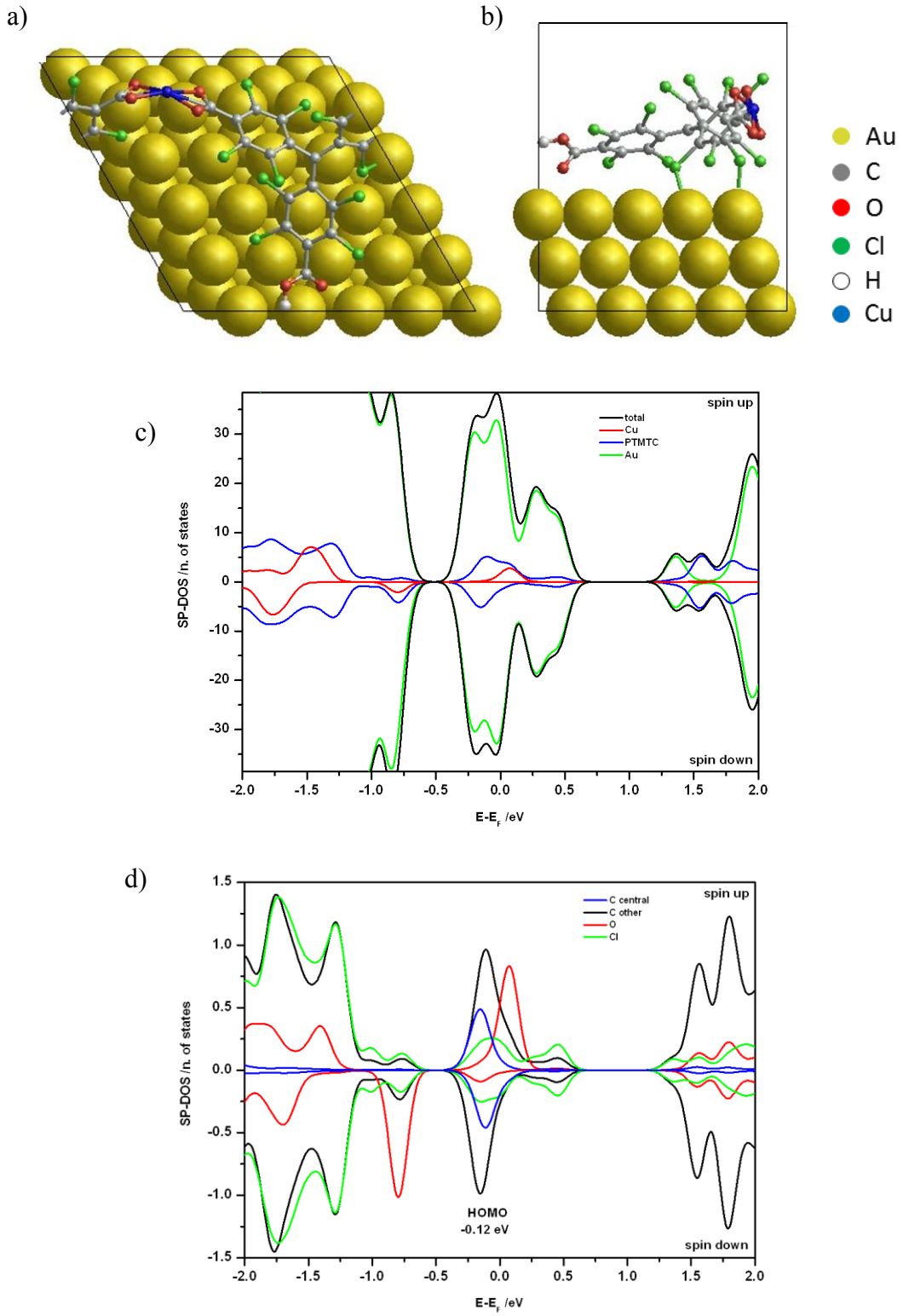

Figure SI.4. Optimized geometry for a PTMTC-Cu unit at a 15° angle to the unreconstructed Au(111) surface; a) top view; b) side view. c) SP-DOS diagrams for Au, Cu, PTMTC and for the whole system. d) Decomposed PTMTC SP-DOS diagram.

Since in the proposed model the copper atom is raised with respect to the surface, interaction between the PTMTC-Cu unit and the gold surface is expected to occur only through the chlorine atoms closer to the surface; these are the chlorine atoms in the *ortho* position with respect to the carbon atom connected to $C_{central}$, belonging to the two phenyl rings sharing the copper atom. The third part of the molecule has the plane of the phenyl ring more parallel to the surface; therefore its chlorine atoms are too far away to successfully interact with the gold surface. Spin up and spin down states for the whole system (Figure SI.4c) are almost totally symmetric, being dominated by the states of the gold surface; there is, however, some asymmetry just below the Fermi level due to the presence of both PTMTC and copper states. The decomposed SP-DOS diagram for the PTMTC molecule (Figure SI.4d) shows that the asymmetry on the molecular spin states is determined by the contributions from oxygen states interacting with copper at *ca.* 0.07 eV in the up state and *ca.* -0.8 eV in the down state. Oxygen states appear to be similar to those of PTMTC-Cu (Figure SI.2b), where charge transfer from oxygen to copper is thought to happen. Moreover, because of the adsorption geometry, copper states are expected to interact with the PTMTC carboxylic group only, not with the gold states. Both the up and down states of the chlorine atoms closest to the surface overlap successfully with the gold states; the chlorine states below the Fermi level are very intense for both the isolated PTMTC molecule and the PTMTC-Cu unit. However, due to the interaction with the gold, charge is transferred from the gold states at *ca.* -1.01 and *ca.* 0 eV to the PTMTC and new empty levels are created at *ca.* 0.45 eV. Spin up and down states of $C_{central}$ and the rest of the carbon atoms align with the gold states around the Fermi level. In particular, the down shift of the spin down state implies charge transfer from the surface to the PTMTC. In this configuration, the spin states associated with $C_{central}$ and C_{other} appear to be symmetric and the PTMTC-Cu unit might lose its radical character, even though some excess of spin due to the interaction of the carboxylic group with the copper atom still exist. This observation strengthens the hypothesis of the carboxylic group not delocalizing in an effective way with the rest of the PTMTC aromatic system.

SI.2.4 PTMTC-Cu normal to the Au(111) surface.

Figure SI.5 shows the optimized geometry for a PTMTC-Cu unit standing upright on the unreconstructed Au(111) surface. This adsorption configuration is suggested by appearance, orientation and dimensions of the molecular features, as in the STM image reported in Figure 4 main text, and well agrees with the vibrations observed in the HREEL spectrum of upright molecules, as in Figure 2 curve b. The gold slab consists of three layers of 3 × 5 gold atoms; a vacuum gap corresponding to 15 gold layers was used to separate the slabs in the vertical direction. In this configuration the interaction between the PTMTC-Cu unit and the gold surface is thought to occur through the copper atom. Oxygen states of the carboxylate group overlap with copper atom states at *ca.* -0.45, -0.15, 0.06, 0.39 eV in the up state and at *ca.* -0.26 and *ca.* 0.06 eV in the down state. The interaction between the PTMTC-Cu unit and the Au(111) surface is due to the overlap of oxygen, copper and gold states at *ca.* 0.39 eV in the up state and at *ca.* -0.26 and *ca.* 0.06 eV in the down state. In the spin up state, the shoulder present at *ca.* -0.46 eV on the $C_{central}$ and C_{other} curves, might account for some charge transfer, however, the superposition between the sates seems never to be much effective. In fact, although with a wider full width at half maximum and a tail that crosses the Fermi level, $C_{central}$ and C_{other} states are once again asymmetric. A SOMO level is thought to be present at *ca.* -0.25 eV (up state) with contributions mainly due to $C_{central}$, C_{other}, whereas the contribution form oxygen does not seem to be so important. Chlorine states appear to be similar to those calculated for the isolated molecule and the PTMTC-Cu unit, implying that the chlorine atoms are not involved in interactions with either the copper atom or the gold surface. The down-LUMO state at *ca.* 0.89 eV has roughly the same ‘composition’ as the one of the free molecule. Δ(SOMO-LUMO) = 1.14 eV is calculated.

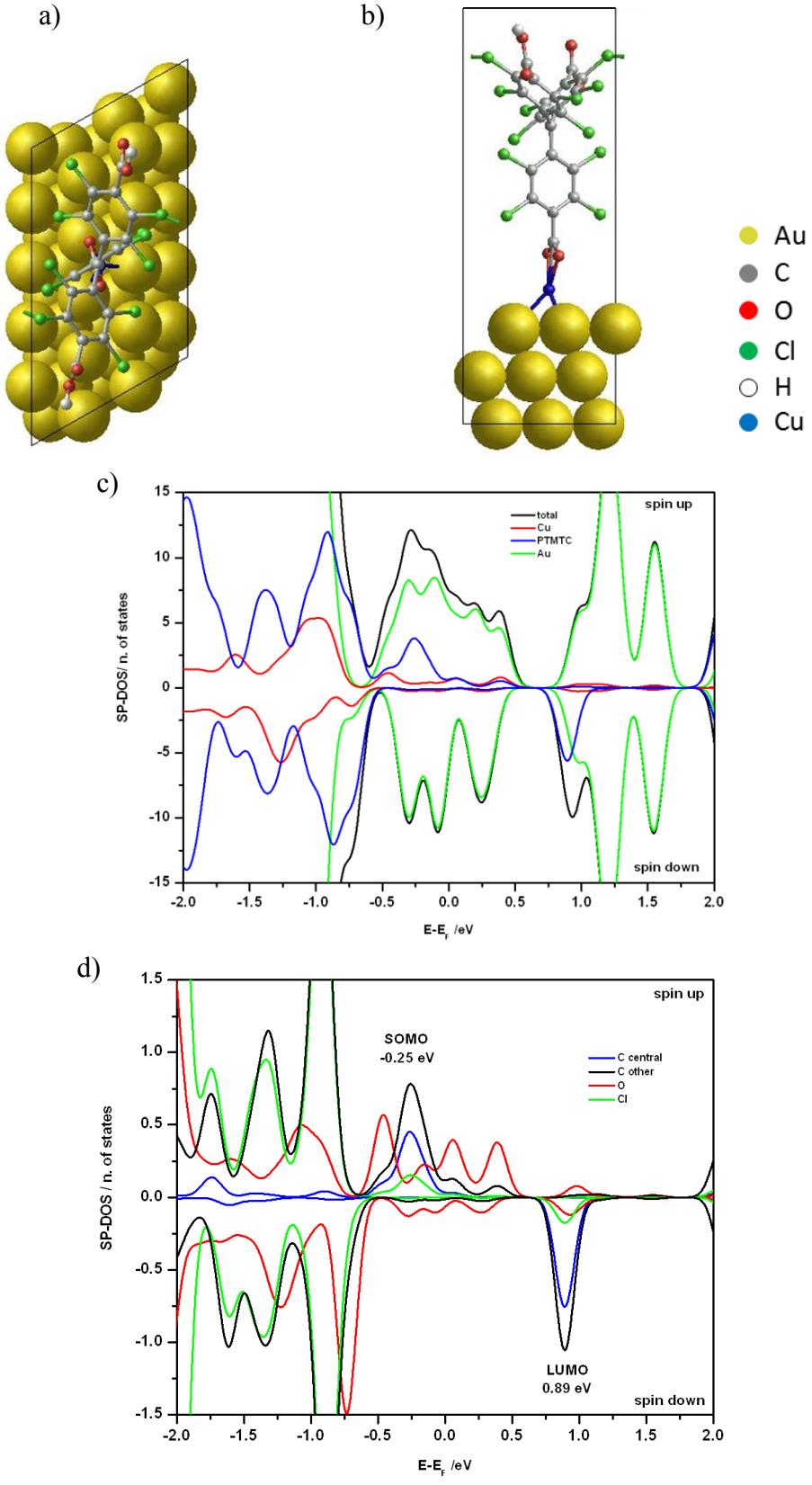

Figure SI.5. Optimized geometry for a PTMTC-Cu unit normal to the unreconstructed Au(111) surface; a) top view; b) side view. c) SP-DOS diagrams for Au, Cu, PTMTC and for the whole system; d) decomposed PTMTC SP-DOS diagram.

SI.3 – Additional STM images

Figure SI.6 shows some additional STM images, recorded after annealing to *ca.* 350 K. Nominal Cu coverage *ca.* 0.2 ML. Scanning parameters: -1.325 V, 0.2 nA; a) 500 × 500 nm^2; b) 500 × 500 nm^2; c) 180 × 180 nm^2; d) 100 × 100 nm^2.

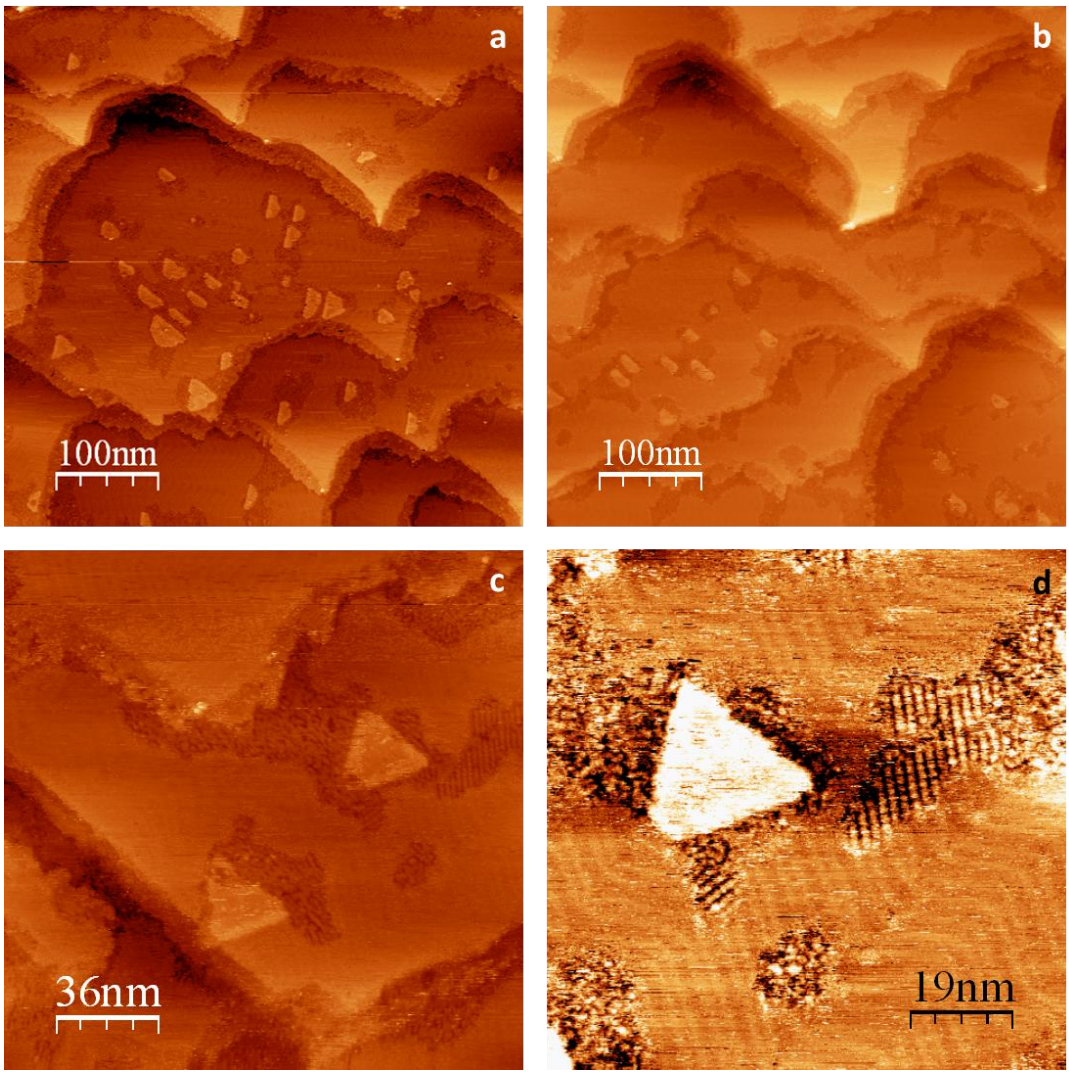

References

1) F. Grillo, V. Mugnaini, M. Oliveros, S. M. Francis, D. J. Choi, M. V. Rastei, L. Limot, C. Cepek, M. Pedio, S. T. Bromley, N. V. Richardson, J. P. Bucher, and J. Veciana, *J. Phys. Chem. Lett.* 2012, **3**, 1559.

2) I. Horcas, R. Fernandez, J. M. Gomez-Rodriguez, J. Colchero, J. Gomez-Herrero and A. M. Baro, *Rev. Sci. Instrum.* 2007, **78**, 013705.

3) B. G. Frederick, G. L. Nyberg and N. V. Richardson, *J. Electron Spectrosc. Relat. Phenom.* 1993, **64/65**, 825; B. G. Frederick and N. V. Richardson, *Phys. Rev. Lett.* 1994, **73**(5), 772.

4) Gaussian 03, Revision E.01; M. J. Frisch, G. W. Trucks, H. B. Schlegel, G. E. Scuseria, M. A. Robb, J. R. Cheeseman, J. A. Montgomery, Jr., T. Vreven, K. N. Kudin, J. C. Burant, J. M. Millam, S. S. Iyengar, J. Tomasi, V. Barone, B. Mennucci, M. Cossi, G. Scalmani, N. Rega, G. A. Petersson, H. Nakatsuji, M. Hada, M. Ehara, K. Toyota, R. Fukuda, J. Hasegawa, M. Ishida, T. Nakajima, Y. Honda, O. Kitao, H. Nakai, M. Klene, X. Li, J. E. Knox, H. P. Hratchian, J. B. Cross, V. Bakken, C. Adamo, J. Jaramillo, R. Gomperts, R. E. Stratmann, O. Yazyev, A. J. Austin, R. Cammi, C. Pomelli, J. W. Ochterski, P. Y. Ayala, K. Morokuma, G. A. Voth, P. Salvador, J. J. Dannenberg, V. G. Zakrzewski, S. Dapprich, A. D. Daniels, M. C. Strain, O. Farkas, D. K. Malick, A. D. Rabuck, K. Raghavachari, J. B. Foresman, J. V. Ortiz, Q. Cui, A. G. Baboul, S. Clifford, J. Cioslowski, B. B. Stefanov, G. Liu, A. Liashenko, P. Piskorz, I. Komaromi, R. L. Martin, D. J. Fox, T. Keith, M. A. Al-Laham, C. Y. Peng, A. Nanayakkara, M. Challacombe, P. M. W. Gill, B. Johnson, W. Chen, M. W. Wong, C. Gonzalez, J. A. Pople, Gaussian, Inc., Wallingford CT, 2004.

5) G. Kresse and J. Hafner, *Phys. Rev. B.* 1993, **47**, 558; G. Kresse and J. Furthmüller, *Phys. Rev. B.* 1996, **54**, 11169; G. Kresse and J. Hafner, *Phys. Rev. B.* 1994, **49**, 14251.

6) J. P. Perdew, K. Burke and Y. Wang, *Phys. Rev. B.* 1996, **54**, 16533.

7) P. E. Blöchl, *Phys. Rev. B.* 1994, **50**, 17953.

8) J. M. Soler, E. Artacho, J. D. Gale, A. Garcia, J. Junquera, P. Ordejon and P. Sanchez-Portal, *J. Phys.: Condens. Matter*, 2002, **14**, 2745.

9) J. P. Perdew and K. Burke, *Phys. Rev. Lett.* 1996, **77**, 3865.

10) O. F. Sankey and D. J. Niklewski, *Phys. Rev. B.* 1989, **40**, 3979.

11) N. Troullier and J. L. Martins, *Phys. Rev. B.* 1991, **43**, 1993.

12) S. García-Gil, A. García, N. Lorente and P. Ordejón, *Phys. Rev. B.* 2009, **79**, 075441.

13) Y. -H. Lu, L. Shi, C. Zhang and Y. -P. Feng, *Phys. Rev. B.* 2009, **80**, 233410.